Title
A Computational Assay that Explores the Hemagglutinin/Neuraminidase Functional Balance Reveals the Neuraminidase Secondary Site as a Novel Anti-Influenza Target.

Journal
ACS central science, 4(11)

ISSN
2374-7943

Authors
Amaro, Rommie E
Ieong, Pek U
Huber, Gary
et al.

Publication Date
2018-11-01

DOI
10.1021/acscentsci.8b00666

Peer reviewed

ACS central science

Research Article

Cite This: ACS Cent. Sci. 2018, 4, 1570−1577

http://pubs.acs.org/journal/acscii

A Computational Assay that Explores the Hemagglutinin/Neuraminidase Functional Balance Reveals the Neuraminidase Secondary Site as a Novel Anti-Influenza Target

Rommie E. Amaro,*[,†] Pek U Ieong,[†] Gary Huber,[†] Abigail Dommer,[†] Alasdair C. Steven,[‡] Robin M. Bush,[§] Jacob D. Durrant,*[,∥] and Lane W. Votapka*[,⊥]

[†]Department of Chemistry and Biochemistry, University of California, San Diego, La Jolla, California, United States

[‡]Structural Biology Laboratory, National Institutes of Health, Bethesda, Maryland, United States

[§]Department of Ecology and Evolutionary Biology, University of California, Irvine, Irvine, California, United States

[∥]Department of Biological Sciences, University of Pittsburgh, Pittsburgh, Pennsylvania, United States

[⊥]Department of Chemistry, Point Loma Nazarene University, San Diego, California, United States

Supporting Information

ABSTRACT: Studies of pathogen−host specificity, virulence, and transmissibility are critical for basic research as well as for assessing the pandemic potential of emerging infectious diseases. This is especially true for viruses such as influenza, which continue to affect millions of people annually through both seasonal and occasional pandemic events. Although the influenza virus has been fairly well studied for decades, our understanding of host-cell binding and its relation to viral transmissibility and infection is still incomplete. Assessing the binding mechanisms of complex biological systems with atomic-scale detail is challenging given current experimental limitations. Much remains to be learned, for example, about how the terminal residue of influenza-binding host-cell receptors (sialic acid) interacts with the viral surface. Here, we present an integrative structural-modeling and physics-based computational assay that reveals the sialic acid association rate constants (k_{on}) to three influenza sites: the hemagglutinin (HA), neuraminidase (NA) active, and NA secondary binding sites. We developed a series of highly detailed (atomic-resolution) structural models of fully intact influenza viral envelopes. Brownian dynamics simulations of these systems showed how structural properties, such as stalk height and secondary-site binding, affect sialic acid k_{on} values. Comparing the k_{on} values of the three sialic acid binding sites across different viral strains suggests a detailed model of encounter-complex formation and indicates that the secondary NA binding site may play a compensatory role in host-cell receptor binding. Our method elucidates the competition among these sites, all present on the same virion, and provides a new technology for directly studying the functional balance between HA and NA.

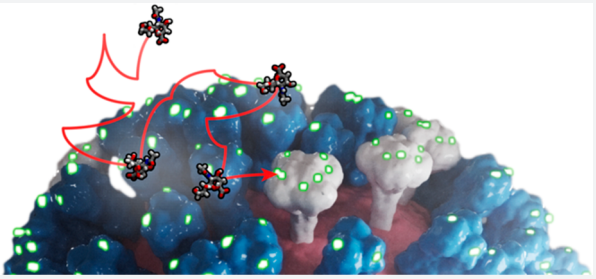

INTRODUCTION

The influenza virus is a negatively stranded RNA virus that encapsulates its cargo with a host-derived lipid bilayer. The two surface glycoproteins embedded in this bilayer, hemagglutinin (HA) and neuraminidase (NA), have complementary functions. According to the accepted paradigm, HA facilitates viral entry, and NA promotes viral release by cleaving host-cell receptors.[1,2] Both NA and HA bind to sialic acid (SIA), a common physiological monosaccharide with a nine-carbon backbone[3,4] and the terminal residue on the host-cell receptors to which the influenza virus binds. These two key glycoproteins and their host-cell receptors are known to play roles in influenza virulence and transmissibility. For example, HA from human influenza strains prefers binding to glycan receptors with a terminal α2,6 SIA linkage; in contrast, HA from the avian strains preferentially recognizes the α2,3 SIA linkage.[5] Sialoglycans attached to the glycoproteins also help evade antibody detection by masking epitopes.[6] The functional equilibrium between HA and NA has also long been known to impact the fitness, transmissibility, infectivity, and virulence of the virus.[5] Wagner et al. showed that an increase of HA affinity for SIA must be counterbalanced with an increase in NA activity to maintain effective replication.[7] A proper HA/NA functional balance is also critical for human-to-human transmission and for transmission across the species barrier.[8]

Little is known about a secondary hemagglutination (SIA-binding) site adjacent to the primary NA sialidase (enzymatic) site,[9−11] though that site is likely to impact the HA/NA functional balance. Previously, Sung et al. investigated the NA secondary site using Brownian dynamics (BD) simulations of SIA binding to individual (isolated) NA glycoproteins.[12]

Received: September 20, 2018
Published: November 9, 2018

DOI: 10.1021/acscentsci.8b00666
ACS Cent. Sci. 2018, 4, 1570−1577

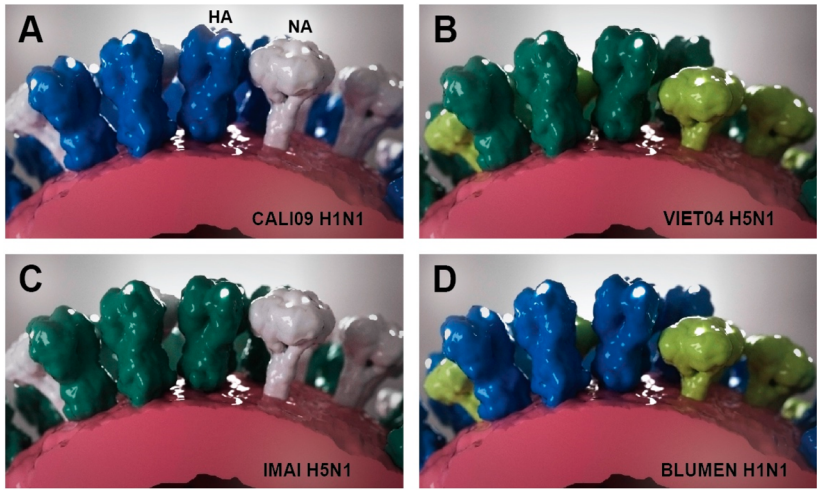

Figure 1. An illustration of the atomic-resolution viral-surface models, shown with reduced resolution to illustrate differences in the NA stalk heights. 09H1 and H5 are colored in blue and green, respectively. 09N1 and avian N1 are colored in white and yellow, respectively. (A) The wild-type H1N1 virus (long-stalk NA). (B) The H5N1 virus with a short-stalk H1N1 NA. (C) The reassortant H5N1 virus studied by Imai et al.[25] (D) The reassortant H1N1 virus studied by Blumenkrantz et al.[24]

Typically BD simulations treat solutes as rigid bodies that are free to tumble and translate (diffuse) through a continuum solvent, driven by electrostatic and stochastic forces that represent the interactions with the solvent molecules. Because most of the details of the solvent and solute are greatly simplified, simulations can be performed much more quickly while still capturing important features of the receptor−ligand interaction. These simulations can reveal second-order complex-encounter association constants via the Northrup-Allison-McCammon formalism,[13] in which the ligand is started on a sphere surrounding the receptor, and a trajectory is generated and terminated upon binding or escaping to a larger surrounding sphere. The proportion of trajectories that bind rather than escape can be used to compute the k_{on}. Knowledge of the k_{on} is important for understanding the kinetics of molecular-recognition events;[14] in the case of influenza, characterizing how SIA encounters or is driven toward the various NA binding sites gives insight into how the virus forms precatalytic "encounter" complexes, potentially providing new opportunities for drug development.

Sung et al. predicted that (1) SIA binding to the NA secondary site in the circulating pandemic H1N1 strain is possible, despite a bioinformatics analysis that speculated otherwise,[15] and (2) SIA association with the H1N1 strain is slower than to the highly pathogenic H5N1 avian strain. Both predictions were later confirmed experimentally by Lai et al.[16] through saturation transfer difference (STD) nuclear magnetic resonance (NMR) on isolated NAs. Together, these single-glycoprotein studies yield new insights into the association of sialic acid with its various NA sites, with the simulations offering mechanistic details not possible with experiments alone. However, these studies did not include HA, which could potentially compete for drug or host-cell−receptor binding. Thus, they provided limited insight into in vivo SIA binding, which involves both HA and NA active sites in the context of a whole viral surface.

Assessing the HA/NA functional balance in physical viruses with atomic-level detail is currently experimentally intractable. Furthermore, experimental assays typically test HA or NA in isolation, and their results cannot be directly correlated with each other, because different methods are used for the individual studies.[17] On the one hand, ethical concerns or the possibility of viral escape also limit some experiments.[18] "Computational assays," on the other hand, are not subject to the same limitations.[19] With sufficient experimental integration and validation, computational assays can extend and enrich our understanding of complex phenomena beyond what is possible experimentally.[20] In this work, we devise a computational assay that allows the time-dependent study of structurally realistic viral surfaces and their interactions with small molecules.

We sought to mimic a series of studies that have investigated the HA/NA functional balance and its impact on transmissibility. We created two in silico influenza-coat models based on known clinical isolates (Figure 1). The VIET04 model represents the highly pathogenic avian influenza (A/Vietnam/1203/2004), which has low transmissibility.[21] The CALI09 model represents the 2009 pandemic flu (A/California/04/2009) that resulted in ∼60.8 million cases.[22]

We also created two in silico models based on lab-created strains (Figure 1). Blumenkrantz et al. used reverse genetics to replace the NA of A/California/04/2009 (CALI09) with the NA of A/Vietnam/1203/2004 (VIET04), which includes a 20-amino acid stalk deletion correlated with limited mammalian viral replication[23] and transmission.[24] Blumenkrantz et al. showed that their construct has a reduced ability to cleave complex sialoglycan substrates and that it exhibits reduced viral transmissibility among ferrets, the mammalian model for human influenza infection. We call our model of this construct "BLUMEN" after the group that performed the NA replacement. Imai et al. also built a reassortant flu virus by swapping the H1 gene in the CALI09 virus with the H5 gene from H5N1.[25] This construct, which we call "IMAI," could have been a potential public health hazard, but it was found to be not transmissible.[25]

We created four atomic-resolution models of these constructs using an integrative modeling approach. To build individual models of membrane-bound NA and HA glycoproteins,[26] we used published crystallographic models,[27−29] homology modeling,[30,31] and protein−protein docking.[32−35] To build models of entire influenza viral surfaces, we used these single-glycoprotein models together with new atomistic membrane-building tools[36] and cryoelectron tomography (cryoET) of a whole influenza

DOI: 10.1021/acscentsci.8b00666
ACS Cent. Sci. 2018, 4, 1570−1577

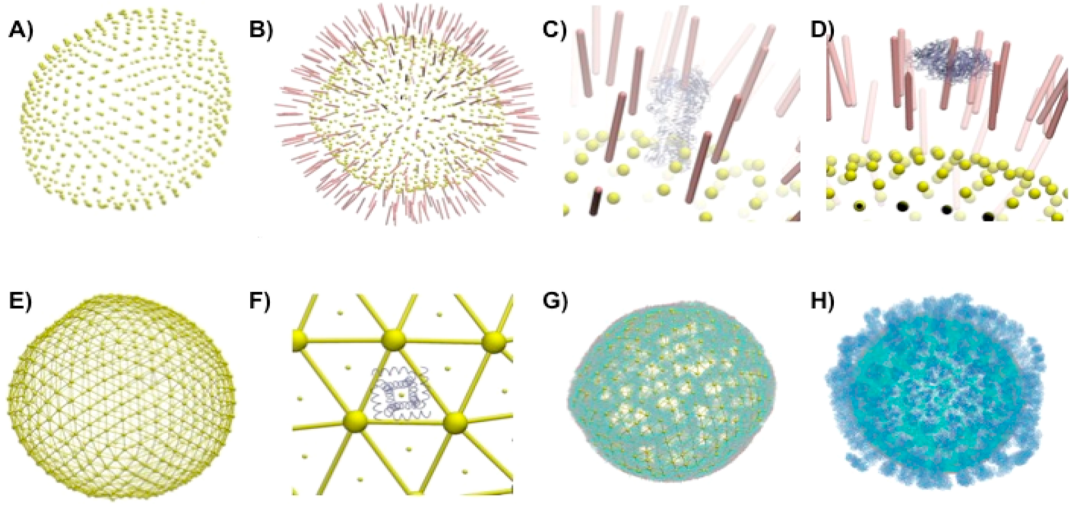

Figure 2. Virion reconstruction. (A) The asymmetrical virus membrane represented as points (from the tomographic data). (B) The proteins within the tomographic map are represented as vectors. (C) HAs are positioned according to their vectors. (D) NAs are similarly positioned. (E) The lipid envelope is constructed through surface meshing via tessellation. (F) The M2 ion channels are inserted randomly into the membrane construct. (G) All-atom lipid molecules are added to the individual triangles that represent the membrane. (H) The full influenza viral surface.

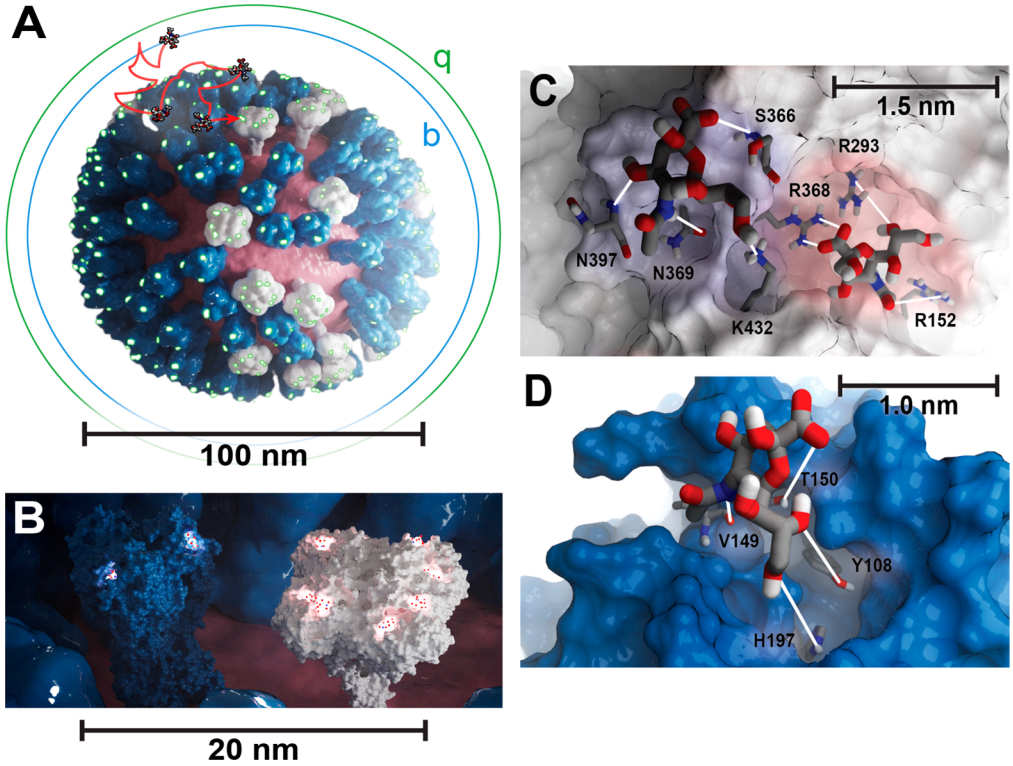

Figure 3. An atomic-resolution virtual model of the viral envelope derived from integrative modeling. (A) The whole viral envelope is shown, with HAs in blue, NAs in white, and membrane in pink. Glowing green points on glycoproteins indicate SIA binding sites. SIA is shown diffusing from the b-surface (starting coordinate) toward the virus or escaping to the q-surface. If SIA escapes, the simulation ends. (B) Close-up of HA (blue) and NA (white), in more detail. SIA binding sites are shown with glowing red and blue points. (C) The encounter-complex definitions of SIA (shown in sticks, illustrated with polar hydrogens) bound to the NA-secondary (blue shading on white surface) and NA-active (red shading on white surface) sites. Atom−atom interactions between the glycoprotein and SIA are visible. (D) The encounter-complex definition of SIA bound to the HA receptor binding domain (blue).

virion[37] (Figure 2, Methods). The resulting atomically detailed, three-dimensional models of the viral coat contain HA, NA, and M2 ion channels positioned with realistic density and spatial patterning. To test the sensitivity of our method to the relative orientation and proximity of the glycoproteins on the viral surface, we also created two in silico strains with randomly placed ("homogenized") distributions of NA and HA on the virion. Each virion contains 236 HA trimers (708 monomers) and 30 NA tetramers (120 monomers). The viruses are ∼120 nm in diameter, though the whole structure is slightly aspherical, per the cryoET image used for modeling. Each virion model contains ∼14.5 million atoms, including hydrogen atoms.

DOI: 10.1021/acscentsci.8b00666
ACS Cent. Sci. 2018, 4, 1570−1577

We then performed atomic-scale BD simulations[38] on each of the structural models to study how the HA, NA active, and NA secondary sites compete for SIA association (Figure 3). The framework presented here significantly extends a previous computational assay developed by Sung et al.,[12] which focused on single glycoproteins in isolation. Our new models include the entire viral coat, allowing us to shift away from a single-protein paradigm in favor of a more accurate and complex whole-virus understanding. The BD simulations of our viral-surface constructs allow us to more rigorously study encounter-complex formation and relative rates of SIA association to the different viral sites. It has not been previously possible to quantifiably explore these important determinants of viral replication and transmissibility.

RESULTS AND DISCUSSION

BD simulations allow us to assess the probability of an "encounter complex" forming between two species at a fixed distance from a binding site (i.e., using the "reaction" criteria). We defined separate reaction criteria for the three SIA-binding sites. Three sets of atomic pairs were defined for each site. The reaction criteria for each given site were satisfied (i.e., successful complex formation was "counted") when the distance between any three of the associated atomic pairs fell within 7.5 Å (Table S1). We selected a distance of 7.5 Å, because that cutoff reproduced the experimentally observed k_{on} for SIA binding to the NA active site[39] (Supporting Information). No experimental k_{on} information is available for the binding of SIA to HA, so we used the same distance criteria (7.5 Å) and selected residue pairs by examining a crystal structure of SIA-bound HA. The second-order association rate constant of SIA to a predefined binding site allows us to quantify binding rate constants and enables us to assess how molecular recognition events differ between the HA and NA SIA binding sites among the four strains. Noting that binding and activity in these systems has been experimentally correlated,[40] we here use the rate of encounter-complex formation, k_{on}, as an initial proxy for activity.

Though there are many more HA binding sites on the influenza surface available for SIA binding, the HA k_{on} is significantly slower than the NA k_{on} in all four constructs. The avian H5 HA had the lowest k_{on} values. Avidity, or the binding of complex sialoglycans to multiple HA sites simultaneously, may compensate for the slow rate of association to HA, though this scenario is not tested here. Nevertheless, our finding that the SIA association rates are faster to both the NA sites compared to the HA sites supports published reports that NA also contributes to host-cell receptor binding, either as a result of specific NA mutations[23,41] or binding to the NA secondary site.[4,16,42]

In all four simulated constructs, the rates of SIA encounter-complex formation were faster to both the NA active and secondary sites than to the HA binding site (Figure 4). The systems with the avian short-stalk NA (VIET04 and BLUMEN) had NA-active-site k_{on} values that were slightly slower than the systems with long-stem NA (CALI09 and IMAI), though the differences were within an order of magnitude. At the same time, the two NA-short-stalk systems had NA-secondary-site k_{on} values that were 2 orders of magnitude faster than the k_{on} to the NA active site. These results suggest that the NA secondary site may compensate for the slower rate to the NA active site in the short-stalk NA. The secondary site may act as a general basin of attraction by electrostatically steering SIA to the area of the NA active site, and the increased binding propensity of SIA to an area adjacent to the NA active site area may ultimately promote cleavage.

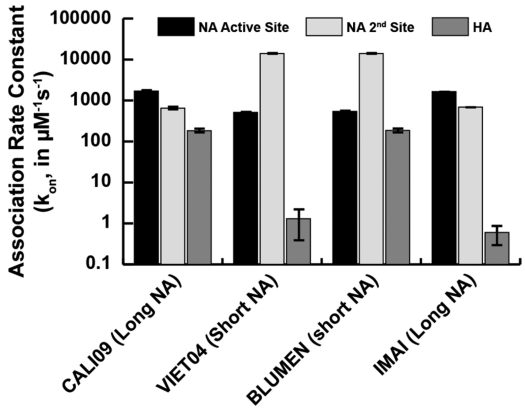

Figure 4. Association rates (log-scale) of SIA to the NA active site, NA secondary site, and HA.

The VIET04, BLUMEN, and IMAI constructs have low or absent transmissibility, while CALI09, the strain that caused the last pandemic, has high transmissibility.[21,24,25,29] Xu et al. found that NA and HA activity must be functionally matched for the emergence of a pandemic (highly transmissible) strain.[8] In the present study, the most transmissible influenza strain, CALI09, has the most similar (i.e., most balanced) association rates to all three SIA sites, with minor differences of 1500 $\mu M^{-1}\cdot s^{-1}$ and within 1 order of magnitude (Figure 4 Table S2). In contrast, our studies suggest that the VIET04 and IMAI HA k_{on} values are comparatively low and that the VIET04 and BLUMAN NA-secondary-site k_{on} values are comparatively high. In these three nontransmissible strains, the k_{on} values among the three SIA-binding sites span 2 to 4 orders of magnitude (Figure 4). These results indicate a large discrepancy in the rates of encounter-complex formation among the three sites. We hypothesize that this imbalance between the SIA binding rates among the three sites may be linked to the low transmissibility of these strains.

Imai et al. found that HPAI H5 had to undergo additional mutations (mainly in the HA receptor-binding domain, or RBD) before transmission in respiratory droplets occurred. Our predicted k_{on} values may reveal the molecular mechanism responsible for this requirement. We hypothesize that the observed HA mutations increase SIA binding to the HA RBD or otherwise compensate for the kinetic imbalance among the three SIA sites present in this strain (e.g., through additional mutations in NA). Our work supports the conclusion of Imai et al. and suggests a molecular-level understanding of how virus mutation and/or reassortment may be linked to transmissibility. In cases where there are substantial differences in the encounter-complex formation rates among the NA active, NA secondary, and HA sites, additional mutations must be acquired to bring the binding sites back into a balanced state.

Our computational assay also allows us to explore open questions about the observed structural organization of NA glycoproteins on the virion surface.[43−49] Clustering (or clumping) of NAs on the surface was observed using anti-NA antibodies first by Compans et al.[50] and again later by Murti and Webster,[51] who reported finding between one and three NA patches per virion. Harris et al.,[37] using the same cryoET data that we use here to construct the experimentally patterned atomic constructs, found both single NA spikes surrounded by HA and multiple patches of NAs. This finding has more recently

DOI: 10.1021/acscentsci.8b00666
ACS Cent. Sci. 2018, 4, 1570−1577

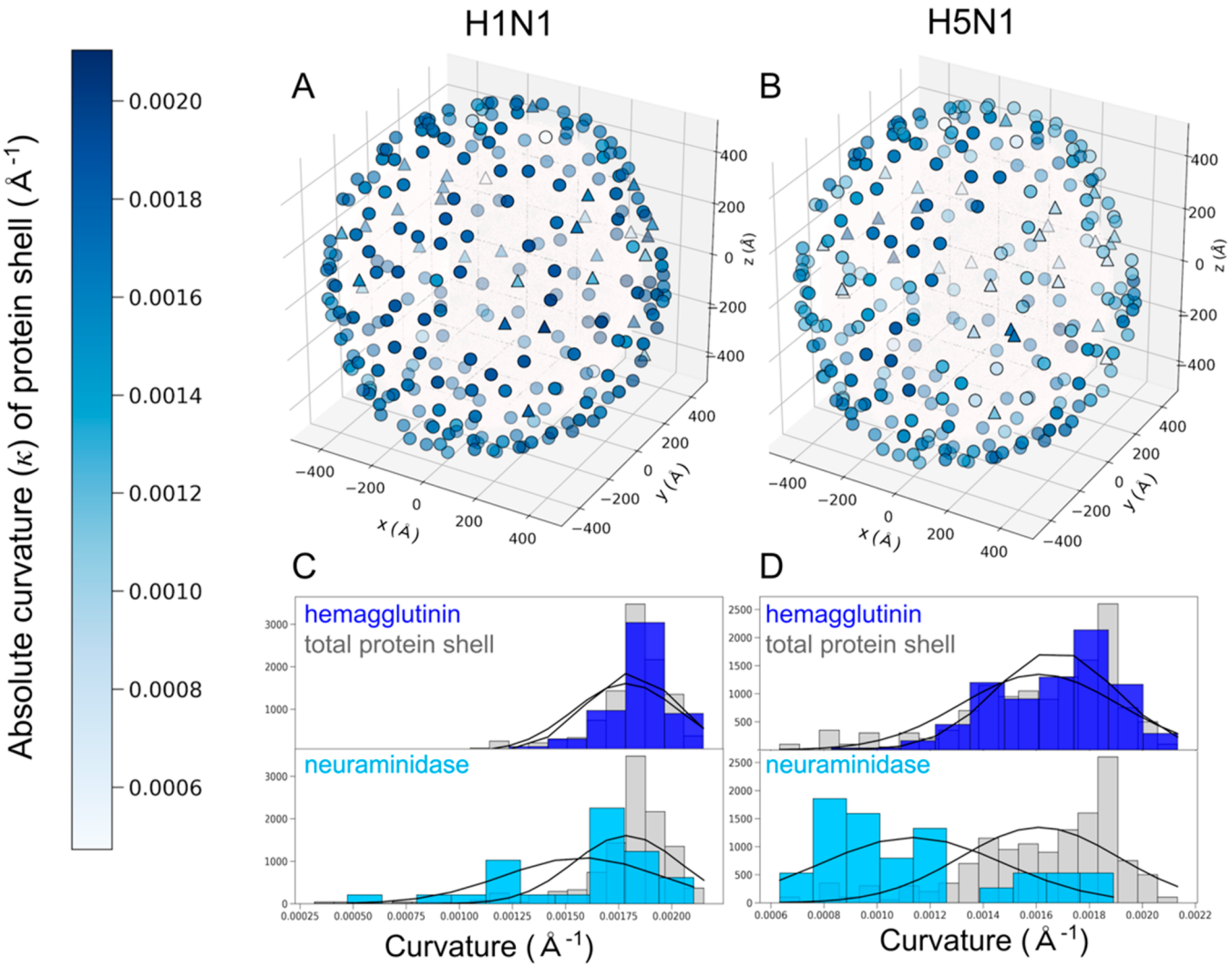

Figure 5. (A, B) H1N1 and H5N1, respectively, plotted by surface protein type and location. Hemagglutinins (circles) and neuraminidases (triangles) are colored by their absolute curvature. Curvature is calculated from fitting a sphere to the surrounding neighborhood of proteins within a 440 Å radius. (C, D) Distributions of curvature values associated with hemagglutinins (top, royal blue) and neuraminidases (bottom, sky blue). H5N1 shows a more significant shift to lower curvatures (flatter surfaces) for neuraminidase compared to the total protein shell than those of H1N1.

been confirmed by Chandla et al.,[52] also via cryoET. Calder et al.[53] and Wasilewski et al.,[54] also using cryoET, reported that the ribonucleoprotein particles (RNP) formed a tapered assembly at one end of the interior of the virus, with the NA glycoproteins occurring in clusters at the end of the virion opposite the RNP attachment. They suggested that NA clusters play a role in viral release from the infected cell by destroying the HA binding to receptors on the cell surface.

Originally, we hypothesized that the rate of sialic acid binding to the available NA sites may be faster to NAs in patches. We tested this hypothesis by creating new strains in silico with randomly placed ("homogenized") distributions of NA and HA and rerunning binding simulations. Our results (Table S4) indicate that the homogenization causes no significant effect on the binding rates between the virus and free floating sialic acid. Further, an analysis of the binding patterns of SIA to the glycoproteins on the experimentally patterned virion (Figure S2) indicates that SIA binds to many different NAs and that once SIA comes within a certain proximity of the NA glycoprotein, it is driven toward binding in a funnel-like fashion (Figures S2 and S3). An analysis of SIA binding with the electrostatics turned off (i.e., electrostatics set to zero in our BD simulations) indicates that the binding of SIA to NA is primarily driven by electrostatics, whereas binding to HA is not (Table S2). Altogether, our results indicate that clustering of NAs does not increase the rate of sialic acid binding to the NA active or secondary sites. Instead, our work effectively substantiates the hypothesis originally put forth by Calder et al.[53] that NA patches likely evolved to enable budding of the virus from the host-cell membrane.

A height analysis of the virion clearly indicates that the regions of NA clusters in the H5N1 (short stalk) viral strain exhibit a depressed area on the viral surface, whereas in the H1N1 (normal NA stalk length), the height differences are significantly less exaggerated (Figure S4). Relatedly, curvature analyses of the whole-virion models similarly indicate that NA clusters in the H5N1 short-stalk strain reduce the curvature of the viral particle in those regions, relative to the H1N1 strain (Figures 5 and S5). Our SIA-binding results indicate that the local surface depressions caused by clusters of NA stalk-deletion glycoproteins do not alter the rates of SIA binding to the available sites, yet it seems plausible that deformations of the virion structure

DOI: 10.1021/acscentsci.8b00666
ACS Cent. Sci. 2018, 4, 1570−1577

due to NA clusters may affect how well the virus binds larger and more structurally complex host cells. Similar to a flattened soccer ball, areas of reduced curvature in the locations of the NA clusters would provide a larger contact area for viral particles to bind to host cells. It seems possible, then, that viral strains with NA stalk deletions may have a slight advantage during the initial binding event to host cells (a scenario not tested here).

CONCLUSIONS

Overall our work suggests a novel pharmaceutical strategy: disrupting the balance between HA and NA activity by targeting the NA secondary site with small-molecule ligands. While inhibitors of NA cleavage (e.g., oseltamivir) will continue to be important, therapeutics targeting the NA secondary site may provide an alternate, potentially less strain-specific approach for combating new influenza variants. Molecular dynamics simulations of the same N1 studied here, combined with computational solvent mapping, have already found regions near the NA secondary site that may be druggable,[26] and Lai et al. have used STD NMR to confirm that SIA analogues bind the NA secondary site.[16] Targeting the secondary site therefore presents a promising unexplored route for disrupting the HA/NA functional balance.

More generally, our work demonstrates the utility of coupling integrative structural models, developed across multiple scales of resolution, to BD simulations. Through the close integration of experiment and simulation, computational assays provide insight into the molecular mechanisms underlying the transmissibility of emerging strains. Our computational assays also enable the systematic interrogation of the structural biology of the influenza virus and the effects that glycoprotein reorganization may have on substrate binding. As our experimental design included both an SIA ligand as well as multiple viral-surface binding sites, it enables a comprehensive and detailed understanding of the competition among multiple sites on the same virion. In this way, large-scale structure-based modeling and physics-based simulation can serve as a powerful tool for investigating the functional balance between HA and NA.

ASSOCIATED CONTENT

Supporting Information

The Supporting Information is available free of charge on the ACS Publications website at DOI: 10.1021/acscentsci.8b00666.

Additional methods information, including figures and tables (PDF)

AUTHOR INFORMATION

Corresponding Authors

*E-mail: ramaro@ucsd.edu. (R.E.A.)
*E-mail: durrantj@pitt.edu. (J.D.D.)
*E-mail: lvotapka100@gmail.com. (L.W.V.)

ORCID

Rommie E. Amaro: 0000-0002-9275-9553
Jacob D. Durrant: 0000-0002-5808-4097

Notes

The authors declare the following competing financial interest(s): REA is a cofounder of, has equity interest in, and is on the scientific advisory board of Actavalon, Inc.

ACKNOWLEDGMENTS

This work was funded in part by the Director's New Innovator Award Program NIH DP2 OD007237 and the National Biomedical Computation Resource (NBCR) through NIH P41 GM103426 to REA. This work was also supported in part by the Intramural Research Program of NIAMS. We thank the NSF for access to the SDSC Comet supercomputer through CHE060073N to REA. We also thank the Center for Research Computing at the University of Pittsburgh for a computing allocation to JDD. We thank Dr. Nathan Baker and the APBS team for assistance with APBS code development. Additional details about the simulations are provided in the Supporting Information.

REFERENCES

(1) Rogers, G. N.; Paulson, J. C. Receptor Determinants of Human and Animal Influenza-Virus Isolates - Differences in Receptor Specificity of the Hemagglutinin-H-3 Based on Species of Origin. *Virology* **1983**, *127* (2), 361−373.

(2) Shtyrya, Y. A.; Mochalova, L. V.; Bovin, N. V. Influenza Virus Neuraminidase: Structure and Function. *Acta Naturae* **2009**, *1* (2), 26−32.

(3) Skehel, J. J.; Wiley, D. C. Receptor Binding and Membrane Fusion in Virus Entry: The Influenza Hemagglutinin. *Annu. Rev. Biochem.* **2000**, *69*, 531−569.

(4) Benton, D. J.; Wharton, S. A.; Martin, S. R.; McCauley, J. W. Role of Neuraminidase in Influenza A(H7N9) Virus Receptor Binding. *J. Virol.* **2017**, *91* (11), e02293−16.

(5) Matrosovich, M.; Tuzikov, A.; Bovin, N.; Gambaryan, A.; Klimov, A.; Castrucci, M. R.; Donatelli, I.; Kawaoka, Y. Early Alterations of the Receptor-Binding Properties of H1, H2, and H3 Avian Influenza Virus Hemagglutinins after Their Introduction into Mammals. *J. Virol* **2000**, *74* (18), 8502−8512.

(6) Wang, C. C.; Chen, J. R.; Tseng, Y. C.; Hsu, C. H.; Hung, Y. F.; Chen, S. W.; Chen, C. M.; Khoo, K. H.; Cheng, T. J.; Cheng, Y. S. E.; et al. Glycans on Influenza Hemagglutinin Affect Receptor Binding and Immune Response. *Proc. Natl. Acad. Sci. U. S. A.* **2009**, *106* (43), 18137−18142.

(7) Wagner, R.; Wolff, T.; Herwig, A.; Pleschka, S.; Klenk, H. D. Interdependence of Hemagglutinin Glycosylation and Neuraminidase as Regulators of Influenza Virus Growth: A Study by Reverse Genetics. *J. Virol.* **2000**, *74* (14), 6316−6323.

(8) Xu, R.; Zhu, X. Y.; McBride, R.; Nycholat, C. M.; Yu, W. L.; Paulson, J. C.; Wilson, I. A. Functional Balance of the Hemagglutinin and Neuraminidase Activities Accompanies the Emergence of the 2009 H1N1 Influenza Pandemic. *J. Virol.* **2012**, *86* (17), 9221−9232.

(9) Laver, W.; Colman, P.; Webster, R.; Hinshaw, V.; Air, G. Influenza Virus Neuraminidase with Hemagglutinin Activity. *Virology* **1984**, *137* (2), 314−323.

(10) Webster, R. G.; Air, G. M.; Metzger, D. W.; Colman, P. M.; Varghese, J. N.; et al. Antigenic Structure and Variation in an Influenza Virus N9 Neuraminidase. *J. Virol.* **1987**, *61* (9), 2910−2916.

(11) Hausmann, J.; Kretzschmar, E.; Garten, W.; Klenk, H.-D. N1 Neuraminidase of Influenza Virus A/FPV/Rostock/34 Has Haemadsorbing Activity. *J. Gen. Virol.* **1995**, *76*, 1719−1728.

(12) Sung, J. C.; Van Wynsberghe, A. W.; Amaro, R. E.; Li, W. W.; McCammon, J. A. Role of Secondary Sialic Acid Binding Sites in Influenza N1 Neuraminidase. *J. Am. Chem. Soc.* **2010**, *132* (9), 2883−2885.

(13) Northrup, S. H.; Allison, S. A.; Mccammon, J. A. Brownian Dynamics Simulation of Diffusion-Influenced Bimolecular Reactions. *J. Chem. Phys.* **1984**, *80* (4), 1517−1526.

(14) Folmer, R. H. A Drug Target Residence Time: A Misleading Concept. *Drug Discovery Today* **2018**, *23* (1), 12−16.

(15) Kobasa, D.; Rodgers, M. E.; Wells, K.; Kawaoka, Y. Neuraminidase Hemadsorption Activity, Conserved in Avian Influenza

DOI: 10.1021/acscentsci.8b00666
ACS Cent. Sci. 2018, 4, 1570−1577

A Viruses, Does Not Influence Viral Replication in Ducks. *J. Virol.* **1997**, *71* (9), 6706−6713.
(16) Lai, J. C. C.; Garcia, J. M.; Dyason, J. C.; Bohm, R.; Madge, P. D.; Rose, F. J.; Nicholls, J. M.; Peiris, J. S. M.; Haselhorst, T.; Von-Itzstein, M. A Secondary Sialic Acid Binding Site on Influenza Virus Neuraminidase: Fact or Fiction? *Angew. Chem., Int. Ed.* **2012**, *51* (9), 2221−2224.
(17) Gaymard, A.; Le Briand, N.; Frobert, E.; Lina, B.; Escuret, V. Functional Balance between Neuraminidase and Haemagglutinin in Influenza Viruses. *Clin. Microbiol. Infect.* **2016**, *22* (12), 975−983.
(18) Fouchier, R. A. Studies on Influenza Virus Transmission between Ferrets: The Public Health Risks Revisited. *mBio* **2015**, *6* (1), 14−17.
(19) Woods, C. J.; Malaisree, M.; Long, B.; McIntosh-Smith, S.; Mulholland, A. J. Computational Assay of H7N9 Influenza Neuraminidase Reveals R292K Mutation Reduces Drug Binding Affinity. *Sci. Rep.* **2013**, *3*, 3561.
(20) Amaro, R. E.; Mulholland, A. J. Multiscale Methods in Drug Design Bridge Chemical and Biological Complexity in the Search for Cures. *Nat. Rev. Chem.* **2018**, *2*, 148.
(21) Gambaryan, A.; Tuzikov, A.; Pazynina, G.; Bovin, N.; Balish, A.; Klimov, A. Evolution of the Receptor Binding Phenotype of Influenza A (H5) Viruses. *Virology* **2006**, *344* (2), 432−438.
(22) Centers for Disease Control and Prevention. CDC Estimates of 2009 H1N1 Influenza Cases, Hospitalizations and Deaths in the United States. https://www.cdc.gov/h1n1flu/estimates_2009_h1n1.htm (accessed Oct 24, 2018).
(23) Mohr, P. G.; Deng, Y. M.; McKimm-Breschkin, J. L. The Neuraminidases of MDCK Grown Human Influenza A(H3N2) Viruses Isolated since 1994 Can Demonstrate Receptor Binding. *Virol. J.* **2015**, *12*, 67.
(24) Blumenkrantz, D.; Roberts, K. L.; Shelton, H.; Lycett, S.; Barclay, W. S. The Short Stalk Length of Highly Pathogenic Avian Influenza H5N1 Virus Neuraminidase Limits Transmission of Pandemic H1N1 Virus in Ferrets. *J. Virol* **2013**, *87* (19), 10539−10551.
(25) Imai, M.; Watanabe, T.; Hatta, M.; Das, S. C.; Ozawa, M.; Shinya, K.; Zhong, G.; Hanson, A.; Katsura, H.; Watanabe, S.; et al. Experimental Adaptation of an Influenza H5 HA Confers Respiratory Droplet Transmission to a Reassortant H5 HA/H1N1 Virus in Ferrets. *Nature* **2012**, *486* (7403), 420−428.
(26) Durrant, J. D.; Bush, R. M.; Amaro, R. E. Microsecond Molecular Dynamics Simulations of Influenza Neuraminidase Suggest a Mechanism for the Increased Virulence of Stalk-Deletion Mutants. *J. Phys. Chem. B* **2016**, *120* (33), 8590−8599.
(27) Liu, J.; Stevens, D. J.; Haire, L. F.; Walker, P. A.; Coombs, P. J.; Russell, R. J.; Gamblin, S. J.; Skehel, J. J. Structures of Receptor Complexes Formed by Hemagglutinins from the Asian Influenza Pandemic of 1957. *Proc. Natl. Acad. Sci. U. S. A.* **2009**, *106* (40), 17175−17180.
(28) Hartmann, M. D.; Ridderbusch, O.; Zeth, K.; Albrecht, R.; Testa, O.; Woolfson, D. N.; Sauer, G.; Dunin-Horkawicz, S.; Lupas, A. N.; Alvarez, B. H. A Coiled-Coil Motif That Sequesters Ions to the Hydrophobic Core. *Proc. Natl. Acad. Sci. U. S. A.* **2009**, *106* (40), 16950−16955.
(29) Li, Q.; Qi, J.; Zhang, W.; Vavricka, C. J.; Shi, Y.; Wei, J.; Feng, E.; Shen, J.; Chen, J.; Liu, D.; et al. The 2009 Pandemic H1N1 Neuraminidase N1 Lacks the 150-Cavity in Its Active Site. *Nat. Struct. Mol. Biol.* **2010**, *17* (10), 1266−1268.
(30) Jacobson, M. P.; Pincus, D. L.; Rapp, C. S.; Day, T. J.; Honig, B.; Shaw, D. E.; Friesner, R. A. A Hierarchical Approach to All-Atom Protein Loop Prediction. *Proteins: Struct., Funct., Genet.* **2004**, *55* (2), 351−367.
(31) Jacobson, M. P.; Friesner, R. A.; Xiang, Z.; Honig, B. On the Role of the Crystal Environment in Determining Protein Side-Chain Conformations. *J. Mol. Biol.* **2002**, *320* (3), 597−608.
(32) Gray, J. J.; Moughon, S. E.; Kortemme, T.; Schueler-Furman, O.; Misura, K. M.; Morozov, A. V.; Baker, D. Protein-Protein Docking Predictions for the CAPRI Experiment. *Proteins: Struct., Funct., Genet.* **2003**, *52* (1), 118−122.
(33) Gray, J. J.; Moughon, S.; Wang, C.; Schueler-Furman, O.; Kuhlman, B.; Rohl, C. A.; Baker, D. Protein-Protein Docking with Simultaneous Optimization of Rigid-Body Displacement and Side-Chain Conformations. *J. Mol. Biol.* **2003**, *331* (1), 281−299.
(34) Chaudhury, S.; Gray, J. J. Conformer Selection and Induced Fit in Flexible Backbone Protein-Protein Docking Using Computational and NMR Ensembles. *J. Mol. Biol.* **2008**, *381* (4), 1068−1087.
(35) Chaudhury, S.; Sircar, A.; Sivasubramanian, A.; Berrondo, M.; Gray, J. J. Incorporating Biochemical Information and Backbone Flexibility in RosettaDock for CAPRI Rounds 6−12. *Proteins: Struct., Funct., Genet.* **2007**, *69* (4), 793−800.
(36) Durrant, J. D.; Amaro, R. E. LipidWrapper: An Algorithm for Generating Large-Scale Membrane Models of Arbitrary Geometry. *PLoS Comput. Biol.* **2014**, *10* (7), e1003720.
(37) Harris, A.; Cardone, G.; Winkler, D. C.; Heymann, J. B.; Brecher, M.; White, J. M.; Steven, A. C. Influenza Virus Pleiomorphy Characterized by Cryoelectron Tomography. *Proc. Natl. Acad. Sci. U. S. A.* **2006**, *103* (50), 19123−19127.
(38) Huber, G. A.; McCammon, J. A. Browndye: A Software Package for Brownian Dynamics. *Comput. Phys. Commun.* **2010**, *181* (11), 1896−1905.
(39) Collins, P. J.; Haire, L. F.; Lin, Y. P.; Liu, J.; Russell, R. J.; Walker, P. A.; Skehel, J. J.; Martin, S. R.; Hay, A. J.; Gamblin, S. J. Crystal Structures of Oseltamivir-Resistant Influenza Virus Neuraminidase Mutants. *Nature* **2008**, *453* (7199), 1258−1261.
(40) Garcia, J. M.; Lai, J. C. C.; Haselhorst, T.; Choy, K. T.; Yen, H. L.; Peiris, J. S. M.; von Itzstein, M.; Nicholls, J. M. Investigation of the Binding and Cleavage Characteristics of N1 Neuraminidases from Avian, Seasonal, and Pandemic Influenza Viruses Using Saturation Transfer Difference Nuclear Magnetic Resonance. *Influenza Other Respir. Viruses* **2014**, *8* (2), 235−242.
(41) Hooper, K. A.; Crowe, J. E.; Bloom, J. D. Influenza Viruses with Receptor-Binding N1 Neuraminidases Occur Sporadically in Several Lineages and Show No Attenuation in Cell Culture or Mice. *J. Virol.* **2015**, *89* (7), 3737−3745.
(42) Wen, Y.-M.; Wang, Y.-X. Biological Features of Hepatitis B Virus Isolates from Patients Based on Full-Length Genomic Analysis. *Rev. Med. Virol.* **2009**, *19* (1), 57−64.
(43) Rossman, J.; Lamb, R. Influenza Virus Assembly and Budding. *Virology* **2011**, *411*, 229−236.
(44) Air, G. M. Influenza neuraminidase. *Influenza Other Respir. Viruses* **2012**, *6*, 245−256.
(45) Noda, T. Native Morphology of Influenza Virions. *Front. Microbiol.* **2012**, *2*, 269.
(46) Nayak, D.; Shivakoti, S.; Balogun, R.; Lee, G.; ZH, Z. Structure, Disassembly, Assembly, and Budding of Influenza Viruses. In *Textbook of Influenza,* 2nd ed.; John Wiley & Sons, Ltd.: Hoboken, New Jersey, 2013.
(47) Russell, R.; Gamblin, S.; Skehel, J. Influenza Glycoproteins: Hemagglutinin and Neuraminidase. In *Textbook of Influenza,* 2nd ed.; John Wiley & Sons, Ltd.: Hoboken, New Jersey, 2013.
(48) Gerber, M.; Isel, C.; Moules, V.; et al. Selective Packaging of the Influenza A Genome and Consequences for Genetic Reassortment. *Trends Microbiol.* **2014**, *22*, 446−455.
(49) Harrison, S. Viral Membrane Fusion. *Virology* **2015**, *479*, 498−507.
(50) Compans, R.; Dimmock, N.; Meier-Ewert, H. Effect of Antibody to Neuraminidase on the Maturation and Hemagglutinating Activity of an Influenza A2 Virus. *J. Virol* **1969**, *4*, 528−534.
(51) Murti, K.; et al. Distribution of Hemagglutinin and Neuraminidase on Influenza Virions as Revealed by Immunoelectron Microscopy. *Virology* **1986**, *149*, 36−43.
(52) Chlanda, P.; Schraidt, O.; Kummer, S.; Riches, J.; Oberwinkler, H.; Prinz, S.; Krausslich, H.; et al. Structural Analysis of the Roles of Influenza A Virus Membrane-Associated Proteins in Assembly and Morphology. *J. Virol.* **2015**, *89*, 8957−8966.
(53) Calder, L.; Wasilewski, S.; Berriman, J.; et al. Structural Organization of a Filamentous Influenza A Virus. *Proc. Natl. Acad. Sci. U. S. A.* **2010**, *107*, 10685−10690.

DOI: 10.1021/acscentsci.8b00666
ACS Cent. Sci. 2018, 4, 1570−1577

(54) Wasilewski, S.; Calder, L.; Grant, T.; Rosenthal, P. Distribution of Surface Glycoproteins on Influenza A Virus Determined by Electron Cryotomography. *Vaccine* **2012**, *30*, 7368−7373.

DOI: 10.1021/acscentsci.8b00666
ACS Cent. Sci. 2018, 4, 1570−1577